Spin-Förster transfer in optically excited quantum dots

Alexander O. Govorov
Department of Physics and Astronomy, Ohio University, Athens, Ohio 45701-2979, USA
(Received 25 September 2004; published 27 April 2005)

The mechanisms of energy and spin transfer in quantum dot pairs coupled via the Coulomb interaction are studied. Exciton transfer can be resonant or phonon-assisted. In both cases, the transfer rates strongly depend on the resonance conditions. The spin selection rules in the transfer process come from the exchange and spin-orbit interactions. The character of energy dissipation in spin transfer is different than that in the traditional spin currents. The spin-dependent photon cross-correlation functions reflect the exciton transfer process. In addition, a mathematical method to calculate Förster transfer in crystalline nanostructures beyond the dipole-dipole approximation is described.

DOI: 10.1103/PhysRevB.71.155323 PACS number(s): 78.67.Hc, 72.25.Fe, 73.21.La

A new field of research, spintronics, studies the principles of manipulation of the spin degree of freedom in solids and molecules,[1] whereas traditional electronics utilizes electric charges. Spintronics is also closely related to quantum information science since the spin is an important element of quantum computing. In most cases, transport of spins in solids and molecular systems comes from transfer or tunneling of charged electrons and, therefore, is accompanied by electric currents. In electronic materials, the electric interactions are often much stronger than the spin-related ones and, therefore, when manipulating charged particles with spins, usual electronics has often obvious advantages compared to spintronics. However, spin may have advantages over charge. In contrast to charge or mass, the angular momentum or spin can be transferred without tunneling or ballistic transport. One particular mechanism of spin transfer without tunneling can occur in optically excited semiconductor quantum dots (QDs); spin-polarized excitons can be transferred between QDs via the long-range noncontact Coulomb interaction.[2] It is important to note that Coulomb (Förster) transfer of spin in QDs becomes possible due to the strong spin-dependent interactions in semiconductors, such as spin-orbit and exchange couplings.[2]

Here we study theoretically the microscopic mechanisms of spin-dependent Förster transfer in a molecule composed of two self-assembled QDs (Figs. 1 and 2). In the typical scheme of Förster transfer,[3] an optically excited exciton in QD1 ("donor") becomes transferred to QD2 ("acceptor") via the Coulomb interaction [Fig. 2(a)]. The traditional methods to observe this transfer are time-resolved photoluminescence (PL) spectroscopy[4] and photon correlations.[5] In the case of resonant transfer in self-assembled QDs, the spin selection rules are determined by the electron-hole exchange interaction in an exciton and by the spin-orbit interaction in the valence band. In a symmetric QD molecule, transfer occurs with conservation of the exciton spin configuration, whereas in QD molecules with broken symmetry, the exciton spin becomes partially lost in the transfer process. The transfer rates exhibit a strong dependence from the exciton energy difference in a QD pair, $\Delta E = E_{exc,dot1} - E_{exc,dot2}$. In the resonant regime $\Delta E \approx 0$, exciton and spin transfer is fast. In the nonresonant regime, transfer can be assisted by acoustic phonons. Again, it strongly depends on ΔE. In contrast to the previous paper on spin transfer,[2] we include here the electron-hole exchange interaction and consider the fine structure of exciton states. In addition, we show that the dipole-dipole approximation is not reliable for the typical interdot distances in experimental structures and describe a method to compute Coulomb matrix elements beyond the dipole approach. Our method is valid when $R \gg a_{\text{lattice}}$, where R is the interdot distance and a_{lattice} is the lattice period. In addition, we note that the Förster transfer mechanism considered in this paper has the electrostatic, near-field nature; this is in contrast to the recent paper on the radiative coupling between QDs.[6]

Experimentally, Förster transfer of excitons can be studied using time-resolve photoluminescence[4] or the photon cross-correlation method.[5,7,8] Experiments on energy transfer in nanostructures were done with colloidal nanocrystals[4] and recently with self-assembled InAs QDs.[5] It is important to note that QDs can also be coupled via tunneling.[9] However, the tunneling amplitude decreases exponentially with increasing the distance between QDs and with the hight of the barrier between QDs. At the same time, the Förster transfer

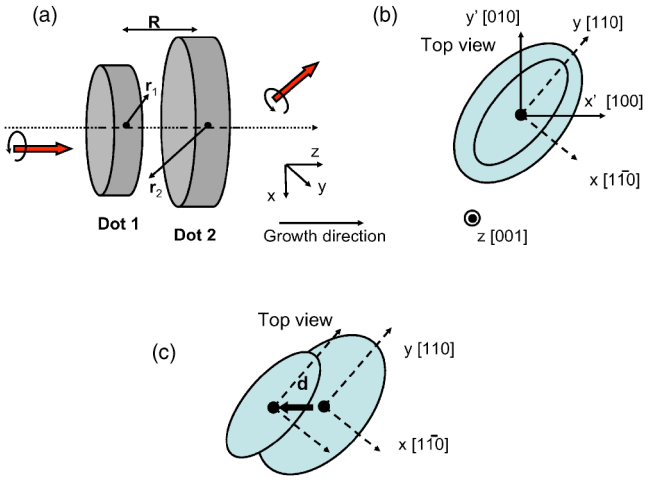

FIG. 1. (Color online) (a) Schematics of the systems of two QDs. (b) Geometry of a pair of self-assembled QDs and the corresponding crystallographic axes. (c) Geometry of two QDs with broken symmetry; the vector **d** describes the shift.

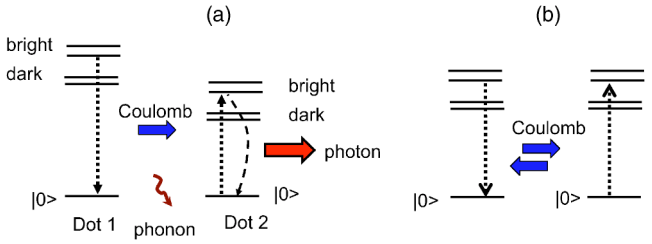

FIG. 2. (Color online) Schematics of transfer processes between two QDs. (a) Phonon-assisted mechanism. (b) Resonant coherent transfer.

rate demonstrates a power law ($\propto R^{-6}$) and is independent of the hight of the potential barrier between QDs. To avoid tunneling in a QD molecule, one can grow an AlGaAs barrier between the QDs or one can use QDs with stronger confinement. Another important factor is that the resonance conditions for Förster and tunneling transfers are different. Therefore it seems to be possible, by using self-organization growth, to design self-assembled QDs with predominantly Förster transfer. The recent experiment[5] indicates that indeed such pairs of QDs with Coulomb-induced coupling can be designed using the self-organization growth method. Another recent experimental paper (Ref. 10) describes the spin-response of colloidal QDs bridged with biomolecules which may assist direct tunnel transport between nanocrystals.[10,11]

The spin current of mobile polarized electrons is accompanied by the electric charge flow. This brings back the old issue of energy dissipation in electronic devices, given by the Joule heat, $Q=\mathbf{jE}$ (here $\mathbf{j}$ is the electric current and $\mathbf{E}$ the driving electric field). In the case of Coulomb-induced transfer between QDs [Figs. 2(a) and 9], the energy dissipation has a different character and comes from phonon-assisted relaxation. The energy loss in this process is equal to the energy level difference in the donor and acceptor QDs: $\Delta E = E_{exc,dot1} - E_{exc,dot2} = \hbar\omega_{ph}$. In such processes, the energy ΔE turns into the phonon energy $\hbar\omega_{ph}$. If a pair of QDs is resonant ($\Delta E \sim 0$), the coupling between QDs can become coherent;[12–14] such a process of spin transfer resembles Rabi oscillations between QDs [Fig. 2(b)]. Coherent spin transfer can occur without dissipation.

The paper is organized as follows: Sec. I describes the model of the QD system, Sec. II includes the results on spin-dependent transfer rates, Sec. III is devoted to the phonon-assisted transfer, and Secs. IV and V are about the photon correlation functions and transfer under strongly resonant conditions.

I. MODEL

We now consider a model of a pair of self-assembled QDs.[5,9,15] Our model incorporates two oblate asymmetric QDs [Figs. 1(a) and 1(b)]; the vertical, z-size of QDs is assumed to be much less than the lateral ones. To model the lateral motion of electrons and holes, we use the harmonic functions[16] with the characteristic lengths, $l_{e(h),x} = \sqrt{\hbar/\omega_x^{e(h)} m_{e(h)}}$ and $l_y^{e(h)} = \sqrt{\hbar/\omega_y^{e(h)} m_{e(h)}}$, where $\omega_{x(y)}^{e(h)}$ are the harmonic-oscillator frequencies for electrons (e) and holes (h), $m_{e(h)}$ are the effective masses of particles, and (x,y) are the in-plane coordinates. The complete envelope functions used below have a form: $\phi_{e,k} = A_{e,k} e^{-x^2/2l_{e,x}^2 - y^2/2l_{e,y}^2} \sin[\pi(z - z_k)/L]$ and $\phi_{h,k} = A_{h,k} e^{-x^2/2l_{h,x}^2 - y^2/2l_{h,y}^2} \sin[\pi(z - z_k)/L]$, where $i=x,y$, $k=1,2$ is the dot number, z_k is the z-coordinate of the center of k-dot, $A_{k,e(h)}$ are the normalizing coefficients, and L is the "vertical" size of QDs. In the following, we will use the system of coordinates (x,y) [Fig. 1(b)] which corresponds to the typical orientation of elongated self-assembled QDs grown on the "001" surface.[17] The lowest excitonic states in QDs responsible for PL are composed of heavy holes and electrons and correspond to the s-like envelope wave function. Taking into account the only heavy-hole wave functions, we can write the spin Hamiltonian of exciton of an individual QD in the following form:[17,18]

$$H_{e\text{-}h}^{spin} = a_z \hat{j}_z \hat{s}_z + \sum_{i=x,y,z} b_i \hat{j}_i^3 \hat{s}_i, \tag{1}$$

where $\hat{s}_i$ is the electron spin matrices and $\hat{s}_i$ are the 2×2 angular-momentum operators of heavy holes. The exchange parameters a_z and b_i depend on a particular QD. By using the operator (1), we find the exciton wave functions and their energies. The bright excitons are composed of the states with $J_{tot} = j_z + s_z = \pm 1$:

$$\psi_x^b = \frac{\left|+\frac{1}{2};-\frac{3}{2}\right\rangle + \left|-\frac{1}{2};+\frac{3}{2}\right\rangle}{\sqrt{2}},$$

$$\psi_y^b = \frac{\left|+\frac{1}{2};-\frac{3}{2}\right\rangle - \left|-\frac{1}{2};+\frac{3}{2}\right\rangle}{\sqrt{2}}, \tag{2}$$

where we used the notation $|s_z; j_z\rangle$. The corresponding energies $\epsilon_x^b = -\left(\frac{3}{4}a_z + \frac{27}{16}b_z\right) + \frac{3}{8}(b_x - b_y)$ and $\epsilon_y^b = -\left(\frac{3}{4}a_z + \frac{27}{16}b_z\right) - \frac{3}{8}(b_x - b_y)$. The lower indexes x,y reflect the character of spin orientation in an exciton and the optical selection rules. In the PL process, the excitons ψ_x^b and ψ_y^b create photons with linear x and y polarizations, respectively. The dark excitons are composed of the states with $J_{tot} = j_z + s_z = \pm 2$:

$$\psi_x^d = \frac{\left|+\frac{1}{2};+\frac{3}{2}\right\rangle + \left|-\frac{1}{2};-\frac{3}{2}\right\rangle}{\sqrt{2}},$$

$$\psi_y^d = \frac{\left|+\frac{1}{2};+\frac{3}{2}\right\rangle - \left|-\frac{1}{2};-\frac{3}{2}\right\rangle}{\sqrt{2}}. \tag{3}$$

Their energies $\epsilon_x^b = -\left(\frac{3}{4}a_z + \frac{27}{16}b_z\right) + \frac{3}{8}(b_x + b_y)$ and $\epsilon_y^b = -\left(\frac{3}{4}a_z + \frac{27}{16}b_z\right) - \frac{3}{8}(b_x + b_y)$. Typically, the two lowest states in the exciton spectrum are dark whereas the two upper ones are bright (Fig. 2). In this model, the normal magnetic field does not lead to mixing between dark and bright states, inducing an additional splitting in the pairs of states. In the limit $B \to \infty$, the wave functions become the states in which the angular momentum is a good quantum number.

The exchange spin-dependent interaction in excitons and the dark-bright energy splitting are quite strong, about 0.5 meV.[17] The other types of interaction in crystalline QDs, inter-dot Coulomb and electron-phonon couplings, can be weaker and we are going to involve them as perturbation. We note that the intradot Coulomb interaction is quite strong, but it does not lead to the interdot exciton transfer; it mostly shifts down the exciton energies. Then, the perturbation Hamiltonian is

$$\hat{H}_{perturb} = U_{Coul}(r_1, r_2) + \hat{H}_{e\text{-}ph} + \hat{H}_{h\text{-}ph}, \tag{4}$$

where U_{Coul} is the interdot Coulomb interaction. The operators $\hat{H}_{e\text{-}ph}$ and $\hat{H}_{h\text{-}ph}$ represent the interaction between acoustic phonons and particles.

II. SPIN-DEPENDENT COULOMB MATRIX ELEMENTS

First we compute the interdot Coulomb matrix elements. The complete set of electron-hole wave functions includes eight states:

$$\left| \pm\frac{1}{2}, \pm\frac{3}{2}; k \right\rangle, \quad \left| \pm\frac{1}{2}, \pm\frac{3}{2}; k \right\rangle, \tag{5}$$

where $k=1,2$ in the QD index. For the one-exciton states, we have $|s_z', j_z'; 1\rangle|0,2\rangle$ and $|0;1\rangle|s_z', j_z'; 2\rangle$; here $|0;k\rangle$ denotes the state of the k-dot without an exciton. Then we write the interdot Coulomb matrix elements as

$$\langle 0;1|\langle s_2, j_2; 2|U_{Coul}|s_1, j_1; 1\rangle|0,2\rangle. \tag{6}$$

In most papers, the matrix elements (6) are calculated within the dipole-dipole approximation which is valid in the limit $R \ll l_{dot}$, where R is the interdot distance and l_{dot} is a characteristic size of QDs ($l_{dot} \sim l_{e(h),x(y)}$). Now we are going to use a method beyond the dipole-dipole approximation. Namely, we are going to use the quantity a_{lattice}/R as a small parameter, where a_{lattice} is the crystal-lattice period. Since, $a_{\text{lattice}} \ll l_{dot}$, our approximation is much better compared with the standard dipole-dipole approximation, $R \gg l_{dot}$. To evaluate the matrix element (6), it is convenient to return to the pure electron representation and to consider two electrons in each QD explicitly:

$$\begin{aligned} M_{|s_1,j_1;dot1\rangle \to |s_2,j_2;dot2\rangle} &= \langle 0;1|\langle s_2, j_2; 2|U_{Coul}|s_1, j_1; 1\rangle|0,2\rangle \\ &= \int d\xi_1 d\xi_1' d\xi_2 d\xi_2' [\Psi_{j_1,1}(\xi_1)\Psi_{-j_1,1}(\xi_1')\Psi_{s_2,2}(\xi_2)\Psi_{j_2,2}(\xi_2')]^* \\ &\times U_{Coul}(r_1, r_1', r_2, r_2')\Psi_{j_1,1}(\xi_1)\Psi_{s_1,1}(\xi_1')\Psi_{j_2,2}(\xi_2)\Psi_{-j_2,2}(\xi_2'), \end{aligned} \tag{7}$$

here $\xi_1=(\mathbf{r}_1, \sigma_1)$ and $\xi_1'=(\mathbf{r}_1', \sigma_1')$ are the spatial and spin coordinates of two electrons in QD1; $\xi_2=(\mathbf{r}_2, \sigma_2)$ and $\xi_2'=(\mathbf{r}_2', \sigma_2')$ are similar coordinates for QD2. $s_{1(2)}$ are the z-components of spin in the conduction band of QD1(2); $j_{1(2)}$ are the z-components of angular momentum of the valence band-electrons. $\Psi_{j_k,k}$ is the electron state in the valence band of the k-QD ($k=1,2, j_k=\pm 3/2$). The function $\Psi_{s_k,k}$ is the state for the conduction band ($s_k=\pm 1/2$). Within the envelope-function approach $\Psi_{j,k}(\xi)=\chi_j(r,\sigma)\phi_{h,i}(r)$ and $\Psi_{s,k}(\xi)=\chi_s(r,\sigma)\phi_{e,i}(r)$, where χ_j and χ_s are the Bloch functions in the valence band (heavy-hole) and in the conduction band, respectively; $\phi_{h(e)}(r)$ is the hole (electron) envelope function. The Förster process involves one electron in QD1 with coordinate r_1 and one electron in QD2 with coordinate r_2 (Fig. 3) and therefore we can integrate over $r_{1(2)}'$. For smooth envelope functions and long-range Coulomb potential, we can rewrite the integral (7) as follows:

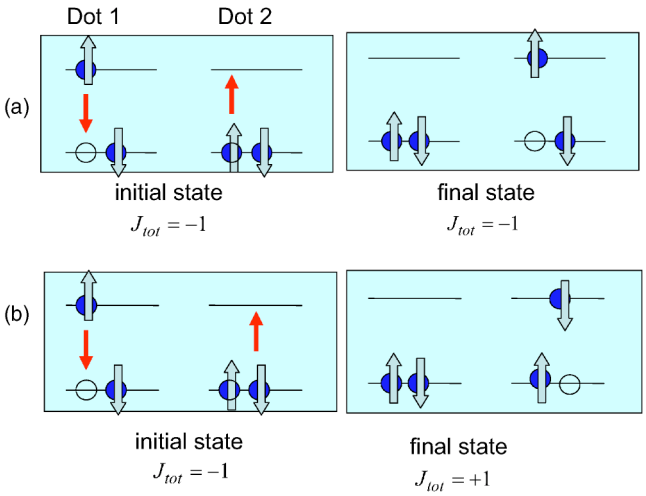

FIG. 3. (Color online) Electron configurations for the initial and final states of the transfer processes with (a) and without (b) conservation of the exciton angular momentum. The process (b) becomes possible in QD pairs with broken symmetry ($d \neq 0$).

$$\begin{aligned} &\sum_{\alpha_1,\alpha_2} \phi_{e,1}(R_{\alpha_1})\phi_{h,1}(R_{\alpha_1})\phi_{e,2}(R_{\alpha_2})\phi_{h,2}(R_{\alpha_2}) \\ &\times \int_{\Omega_{\alpha_1}} \int_{\Omega_{\alpha_2}} d\Delta\xi_1 d\Delta\xi_2 [\chi_{j_1}(\xi_1)^* \chi_{s_2}(\xi_2)^* \\ &\times U_{Coul}(R_{\alpha_1} + \Delta R_{\alpha_1}, R_{\alpha_2} + \Delta R_{\alpha_2})\chi_{s_1}(\xi_1)\chi_{j_2}(\xi_2)], \end{aligned} \tag{8}$$

where the summation is performed over all the unit cells in both QDs; $\alpha_{1(2)}$ are the unit cell indexes; Ω_{α_k} and R_{α_k} are the unit cell volumes and unit cell coordinates, respectively ($k=1,2$). $\Delta\xi_k=(\Delta R_{\alpha_k}, \sigma_k)$, where ΔR_{α_k} is the spatial coordinate relative to the center of the α-cell and σ_k is the spin coordinate. Assuming $a_{\text{lattice}}/l_{dot} \sim a_{\text{lattice}}/R \ll 1$, we expand the Coulomb potential in terms of ΔR_{α_k} and take into account the leading term responsible for the Förster transfer:

$$\begin{aligned} &U_{Coul}(R_{\alpha_1} + \Delta R_{\alpha_1}, R_{\alpha_2} + \Delta R_{\alpha_2}) \\ &= \frac{e^2}{\epsilon} \frac{\Delta R_{\alpha_1} \Delta R_{\alpha_2} - 3[(\Delta R_{\alpha_1} R_{\alpha_1,\alpha_2})(\Delta R_{\alpha_2} R_{\alpha_1,\alpha_2})]/|R_{\alpha_1,\alpha_2}|^2}{|R_{\alpha_1,\alpha_2}|^3}, \end{aligned} \tag{9}$$

where $R_{\alpha_1,\alpha_2}=R_{\alpha_1}-R_{\alpha_2}$. The Coulomb potential was taken in

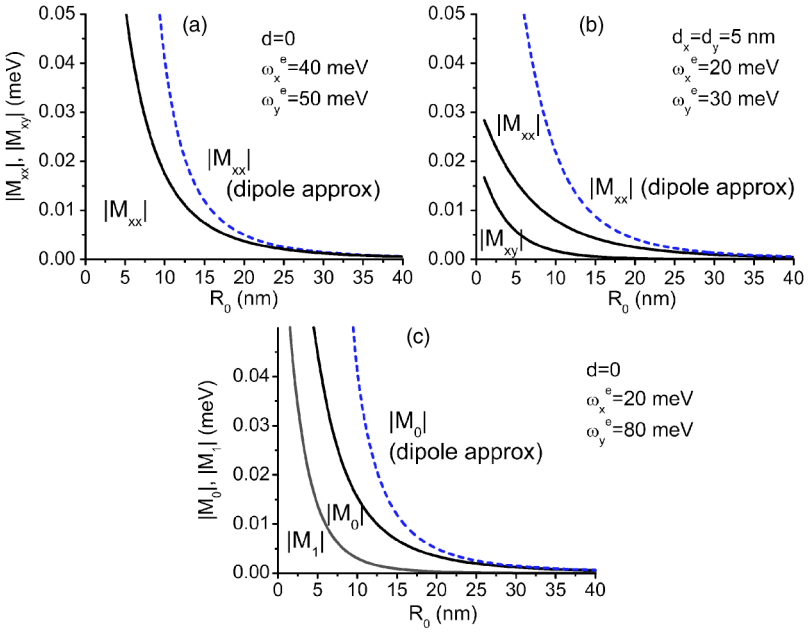

FIG. 4. (Color online) Calculated transfer amplitudes for QD pairs of various parameters and symmetry. a) Transfer amplitudes for $d=0$. $M_{xx}=M_{yy}$ describe the processes with spin conservation; $|M_{xy}|=|M_{yx}|=0$. (b) Transfer amplitudes at $d\neq 0$. (c) Calculated transfer amplitudes M_0 (spin conservation) and M_1 (spin-flip) describing transfer processes at high magnetic fields and $d=0$. In (c) the QDs are strongly asymmetric.

the usual form: $U_{Coul}=e^2/(\epsilon|r_1-r_2|)$. Changing the summation in Eq. (8) to integration, we obtain

$$M_{|s_1,j_1;dot1\rangle\to|s_2,j_2;dot2\rangle} = \frac{e^2}{\epsilon}\int dR_1 dR_2 \phi_{e,1}(R_1)\phi_{h,1}(R_1)\phi_{e,2}(R_2)\phi_{h,2}(R_2) \times \int_{\Omega_1}\int_{\Omega_2} d\Delta\xi_1 d\Delta\xi_2 \Bigg[\chi_{j_1}(\Delta\xi_1)^*\chi_{s_2}(\Delta\xi_2)^* \times \frac{\Delta R_1\Delta R_2 - 3[(\Delta R_1 R_{12})(\Delta R_2 R_{12})]/|R_{12}|^2}{|R_{12}|^3} \times \chi_{s_1}(\Delta\xi_1)\chi_{j_2}(\Delta\xi_2)\Bigg], \quad (10)$$

where $R_{12}=R_1-R_2$ and $\Delta\xi_k=(\Delta R_k,\sigma_k)$. In the next step, we derive the matrix elements for the heavy-hole excitons using the Bloch functions, $\chi_{1/2}=|S\rangle\uparrow$, $\chi_{-1/2}=|S\rangle\downarrow$, $\chi_{+3/2}=(|X\rangle+i|Y\rangle)\uparrow/\sqrt{2}$, $\chi_{-3/2}=(|X\rangle-i|Y\rangle)\downarrow/\sqrt{2}$,

$$M_0 = M_{|s_1=+1/2,j_1=-3/2;dot1\rangle\to|s_2=+1/2,j_2=-3/2;dot2\rangle} = M_{|s_1=-1/2,j_1=+3/2;dot1\rangle\to|s_2=-1/2,j_2=+3/2;dot2\rangle} = E_0\int dR_1 dR_2 F_{cv}(R_1,R_2)\frac{1-\frac{3}{2}\frac{(X_1-X_2)^2+(Y_1-Y_2)^2}{|R_1-R_2|^2}}{|R_1-R_2|^3},$$

$$M_1 = M_{|s_1=+1/2,j_1=-3/2;dot1\rangle\to|s_2=-1/2,j_2=+3/2;dot2\rangle} = M^*_{|s_1=-1/2,j_1=+3/2;dot1\rangle\to|s_2=+1/2,j_2=-3/2;dot2\rangle} = -E_0\int dR_1 dR_2 F_{cv}(R_1,R_2)\frac{3}{2}\frac{[X_1-X_2-i(Y_1-Y_2)]^2}{|R_1-R_2|^5}. \quad (11)$$

Here $E_0=e^2d_0^2/\epsilon$, $F_{cv}(R_1,R_2)=\phi_{e,1}(R_1)\phi_{h,1}(R_1)\phi_{e,2}(R_2)\phi_{h,2}(R_2)$ and $d_0=\langle S|x|X\rangle$. The matrix element $\langle S|x|X\rangle$ can also be written as $-\hbar/(im_0)\times(P_{cv}/E_g)$, where P_{cv} and E_g are the interband optical matrix element and the band gap energy of the bulk crystal, respectively.

The matrix element M_0 describes the transfer process with conservation of spin, whereas M_1 relates to the spin-flip process. The exciton states with $J_{tot}=\pm 2$ have no matrix elements in our model.[19] The transfer processes with bright excitons [Eq. (2)] have the following amplitudes:

$$M_{\psi^b_x,dot1\to\psi^b_x,dot2} = M_0 + \mathrm{Re}[M_1],$$

$$M_{\psi^b_y,dot1\to\psi^b_y,dot2} = M_0 - \mathrm{Re}[M_1],$$

$$M_{\psi^b_x,dot1\to\psi^b_y,dot2} = -i\,\mathrm{Im}[M_1]$$

$$M_{\psi^b_y,dot1\to\psi^b_x,dot2} = i\,\mathrm{Im}[M_1]. \quad (12)$$

The matrix elements (12) strongly depend on symmetry. Especially, it is related to the off-diagonal transfer processes $x\leftrightarrow y$. The off-diagonal amplitudes can be written as

$$M_{\psi^b_x,dot1\to\psi^b_y,dot2} = M^*_{\psi^b_y,dot1\to\psi^b_x,dot2} = -E_0\int dR_1 dR_2 F_{cv}(R_1,R_2) \times \frac{3(X_1-X_2)(Y_1-Y_2)}{|R_1-R_2|^5}. \quad (13)$$

If the double-dot system is symmetric with respect to the inversion operations $R_{1(2)}\to -R_{1(2)}$, $M_1=0$ and the transfer process conserves the linear polarization of excitons, i.e., x-exciton in QD1 turns into x-exciton in QD2 and the same rule is applied to y-excitons. Therefore spin information can be transferred without losses in the system with spatial-

inversion symmetry $R \to -R$. If the dots are shifted with respect to each other in the xy-plane [Fig. 1(c)], spin information in the transfer process becomes partially lost since $M_1 \neq 0$; if the shift d is small, $M_1 \propto d_x d_y$. The calculated amplitudes of various transfer processes are shown in Fig. 4. For both QDs, we used the following parameters: $L=2$ *nm*, $\omega^h_{x(y)} = \omega^e_{x(y)}/3$, $m_e = 0.07 m_0$, and $m_h = 0.25 m_0$. The above parameters are typical for InAs-based QDs.[16]

We note that it is very important to compute the matrix elements beyond the dipole-dipole approach since the amplitudes $x \leftrightarrow y$ vanish within the dipole-dipole approximation. Also, the generalized dipole approach ($R \gg a_{\text{lattice}}$) used in this paper is necessary to obtain reliable numbers for all the matrix elements at interdot distances $R \sim l_{dot}$ which are typical for experiments. The amplitudes of processes with spin-flip, $|\psi^h_x, dot1\rangle \to |\psi^h_y, dot2\rangle$ and $|\psi^h_y, dot1\rangle \to |\psi^h_x, dot2\rangle$, cannot be obtained within the dipole-dipole approach: $\text{Im}[M_1] \propto R^{-5}$ for $R \to \infty$. At the same time, the Förster transfer elements with conservation of exciton spin has the usual asymptotic behavior at $R \to \infty$: $M_0 \propto R^{-3}$.

In a normal magnetic field, the Hamiltonian (1) has an additional term

$$H^{mag}_{e\text{-}h} = \mu_B \left(g_e \hat{s}_z + \frac{g_{h,z}}{3} \hat{j}_z \right) B, \tag{14}$$

where B is the normal magnetic field, and g_e and $g_{h,z}$ are the g factors. The eigenstates of the Hamiltonian in a strong magnetic field are pure states of the total angular momentum: $|s_k = \pm 1/2, j_k = \pm 3/2\rangle$. Thus the transfer matrix elements in the limit $B \to \infty$ are given by Eqs. (11). The transfer process with conservation of spin is given by the element M_0, whereas the spin-flip transfer processes are given be M_1. Again, it is important to stress the role of symmetry for exciton transfer with spin-flip. If the double-dot system is cylindrically symmetric, the spin-flip transfer processes vanish, $M_1 = 0$. In the case of asymmetric QDs, $M_1 \neq 0$. Figure 4 shows the calculated amplitudes for the case $d=0$ and strongly asymmetric QDs. One can see that the spin-flip processes become important at small interdot distances. Again, the dipole approach would not describe such spin-flip effects.

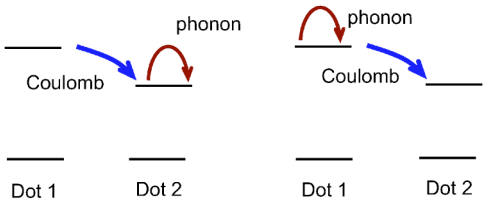

FIG. 5. (Color online) Two contributions to phonon-assisted transfer with different virtual intermediate states.

III. PHONON-ASSISTED COULOMB TRANSFER

In real QD systems, it is very difficult to find QDs with the same exciton energy. Therefore one should involve acoustic phonons to satisfy the energy conservation requirement [Fig. 2(a)]. The operator of exciton-phonon interaction reads[20]

$$\hat{H}_{exc\text{-}ph} = \sum_q \sqrt{\frac{\hbar q}{2\rho V c_{ph}}} [\sigma_e e^{i\mathbf{q}\mathbf{r}_e} (\hat{c}_q + \hat{c}^+_{-q}) + \sigma_h e^{i\mathbf{q}\mathbf{r}_h} (\hat{c}_q + \hat{c}^+_{-q})]. \tag{15}$$

Here $\hat{c}_q$ is the phonon annihilation operator, $r_{e(h)}$ are the electron (hole) coordinates, $c_{ph} = 5.6 \times 10^5$ cm/s is the speed of longitudinal sound, $\sigma_{e(h)} = -8.0$ eV (1.0 eV) are the deformational potentials, and $\rho = 5.3$ g/cm^3 is the crystal mass density. The rate of phonon-assisted transfer includes two second-order processes (Fig. 5):

$$W^{ph}_{dot1,\alpha \to dot2,\alpha'} = \frac{2\pi}{\hbar} \sum_q \left| \frac{\langle dot2|\hat{H}_{exc\text{-}ph}|dot2\rangle \langle dot2|U_{Coul}|dot1\rangle}{\Delta E} + \frac{\langle dot2|U_{Coul}|dot1\rangle \langle dot1|\hat{H}_{exc\text{-}ph}|dot1\rangle}{-\hbar c_{ph}|q|} \right|^2 \delta(\Delta E - \hbar c_{ph}|q|), \tag{16}$$

where $|dot1\rangle = |\alpha;1\rangle|0;2\rangle$ and $|dot2\rangle = |0;1\rangle|\alpha';2\rangle$ denote the states in which an exciton is in QD1 or in QD2, respectively; $\alpha = x,y$ is the spin index of exciton. The notation $|0;k\rangle$ means an empty QD.

Then, the rate (16) is reduced to

$$W^{ph}_{dot1,\alpha \to dot2,\alpha'} = \frac{1}{2\pi\hbar} \frac{|M_{dot1,\alpha \to dot2,\alpha'}|^2}{\Delta E^3} \frac{\hbar q_0^4}{\rho c_{ph}} \times F(q_0)[N(\Delta E) + 1], \tag{17}$$

where $M_{dot1,\alpha \to dot2,\alpha'}$ is the interdot Coulomb matrix element between the excitonic states α and α' given by Eqs. (12) and (13), the index $\alpha = x,y$, $q_0 = \Delta E/(\hbar c_{ph})$, $F(q_0)$ is a function given by an integral, and $N(\Delta E)$ is the Bose distribution function at temperature T.

The rates calculated from Eq. (17) strongly depend on the energy difference ΔE (Fig. 6). At small ΔE and low temperature T, the rate decreases due to the phonon density of states, whereas at large ΔE, it becomes small due to the matrix elements of the function e^{iqr}. The calculated rate is maximum at $\Delta E \sim 2$ meV and is about ns^{-1}. Since the exciton-phonon interaction (15) does not include spin-dependent operators, the spin information is not lost in the phonon-emission process. Therefore the spin-selection rules are given by the Coulomb matrix elements while the phonon matrix elements

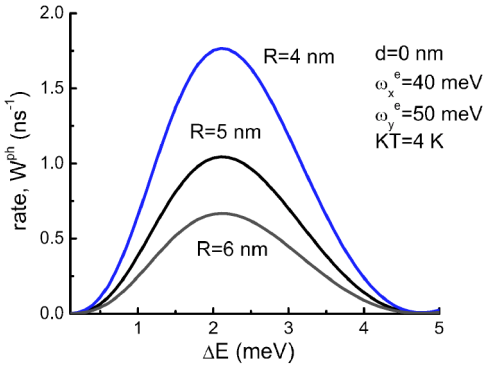

FIG. 6. (Color online) Calculated rates of phonon-assisted transfer as a function of the resonance ΔE at $T=4$ K. The QD pair has inversion symmetry, $d=0$.

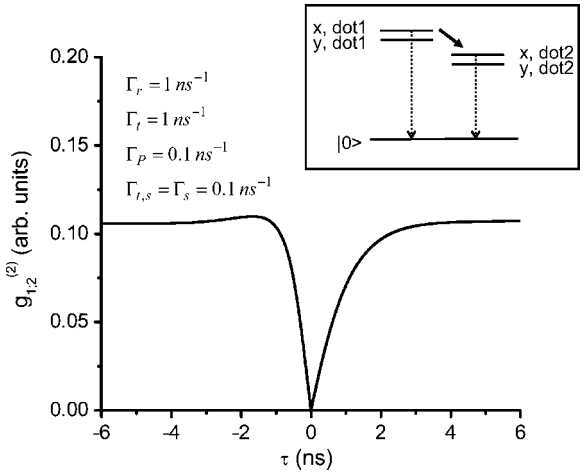

FIG. 7. Calculated cross-correlation functions for a QD pair with one exciton. The correlation function is independent of the spin state of excitons. The parameters of relaxation are shown in the figure and correspond to a QD pair with $R=5$ nm, $d=0$, and $\Delta E \sim 2$ meV. Inset: the energy diagram.

conserve the exciton spin configuration.[21] In a symmetric pair of QDs with $d=0$, the spin of exciton is conserved. However, it is important to note that we have neglected the mixing between heavy and light holes; this mixing together with the electron-phonon interaction can result in an additional spin relaxation. In oblate QDs considered here, our approximation is justified since the heavy hole-light hole mixing is suppressed due to the large slitting between heavy- and light-hole levels in the valence band.

IV. SPIN-DEPENDENT CROSS-CORRELATION FUNCTIONS

Similar to the molecular systems,[8] the coupling between QDs can be seen in the photon correlation measurements.[5] Here we are going to introduce spin-dependent correlation functions for the case of two coupled QDs. The second-order correlation function is defined as $g_{ij}^{(2)}=\langle I_i(t)I_j(t+\tau)\rangle/\langle I_i(t)\rangle \times\langle I_j(t)\rangle$, where $I_i(t)$ is the emission intensity of the i-exciton state. The function $g_{ij}^{(2)}$ is proportional to a number of photon pairs arriving with time interval τ.

The nonlinear dynamics of a double-dot system can be quite complex. For simplicity, we will consider the limit of weak pumping when the biexciton contribution to the density matrix is small. Assuming nonresonant unpolarized excitation of low intensity, we can describe the exciton dynamics with a system of linear equations:

$$\dot{n}_0 = \Gamma_r(n_{x,1} + n_{y,1} + n_{x,2} + n_{y,2}) - 4\Gamma_P n_0,$$

$$\dot{n}_{x,1} = -(\Gamma_r + \Gamma_t + \Gamma_{t,s} + \Gamma_s)n_{x,1} + \Gamma_s n_{y,1} + \Gamma_P n_0,$$

$$\dot{n}_{x,2} = -(\Gamma_r + \Gamma_s)n_{x,2} + \Gamma_{t,s} n_{y,1} + \Gamma_s n_{y,2} + \Gamma_P n_0, \qquad (18)$$

$$\dot{n}_{y,1} = -(\Gamma_r + \Gamma_t + \Gamma_{t,s} + \Gamma_s)n_{x,1} + \Gamma_s n_{x,1} + \Gamma_P n_0,$$

$$\dot{n}_{y,2} = -(\Gamma_r + \Gamma_s)n_{y,2} + \Gamma_{t,s} n_{x,1} + \Gamma_s n_{x,2} + \Gamma_P n_0,$$

where n_0 is the "vacuum" exciton state, $n_{\alpha,k}$ are the numbers of excitons, $\alpha=x,y$ is the type of exciton at $B=0$, and $k=1,2$ is the QD number. The rate Γ_r describes radiative recombination, Γ_t is the energy transfer rate from QD1 to QD2 with conservation of spin, $\Gamma_{t,s}$ is the interdot transfer rate with spin flip, Γ_s is the intradot spin-flip rate, and Γ_P is the pumping rate proportional to the light intensity. This simple model resembles the ones used in Refs. 5 and 22. For our calculations we choose: $\Gamma_t=1\ \mathrm{ns}^{-1}$, $\Gamma_r=1\ \mathrm{ns}^{-1}$, $\Gamma_{t,s}=\Gamma_s=0.1\ \mathrm{ns}^{-1}$, and $\Gamma_P=0.1\ \mathrm{ns}^{-1}$. The pumping rate $\Gamma_P=0.1\ \mathrm{ns}^{-1}$ corresponds to the regime of low intensity ($n_0 \sim 1$). The small phenomenological spin-flip rates are chosen to take into account spin-flip events which are typically slow. The calculated cross-correlation functions are shown in Figs. 7 and 8.

First we describe one-exciton cross-correlation functions $g_{x,1;x,2}^{(2)}$ and $g_{x,1;y,2}^{(2)}$ which turn out to be spin-independent in our model for the weak pumping regime: $g_{x,1;x,2}^{(2)}=g_{x,1;y,2}^{(2)}=g_{1;2}^{(2)}$. The time delay τ is positive when the photon with energy $E_{exc,dot1}$ arrives before the photon with $E_{exc,dot2}$. At $\tau=0$, emission of the photon $E_{exc,dot1}$ projets the system from the state $|dot1,x\rangle$ to the "vacuum" state. Therefore the initial conditions for Eqs. (18) are set as $n_0=1$ and $n_{\alpha,k}=0$. For $\tau>0$, $g_{1;2}^{(2)} \propto n_{x,2}(\tau)=n_{y,2}(\tau)$, where $n_{x(y),2}(\tau)$ are the solutions of Eqs. (18) for the above initial conditions. For $\tau<0$, $g_{1;2}^{(2)} \propto n_{x,1}(\tau)=n_{y,1}(\tau)$. The function $g_{1;2}^{(2)}$ is not symmetric with respect to τ because of directional exciton transfer from QD1 toward QD2. The effective exciton lifetime in QD1 is shorter since an exciton can be transferred to QD2. This is reflected as a faster increase of $g_{1;2}^{(2)}$ at $\tau<0$. In a magnetic field, the cross-correlation functions can become polarization-dependent ($g_{x,1;x,2}^{(2)} \neq g_{x,1;y,2}^{(2)}$) since the resonance conditions can be different for various transfer processes. This can be incorporated in the model through appropriate spin-dependent transfer rates $\Gamma_{t,J_{tot}\to J'_{tot}}$.

Spin transfer processes can be observed using the biexciton lines. Even at small pumping, weak biexciton lines exist. The energy of biexciton lines are redshifted by a few meV and can be distinguished from the one-exciton lines. In addition, the biexciton lines have a quadratic power depen-

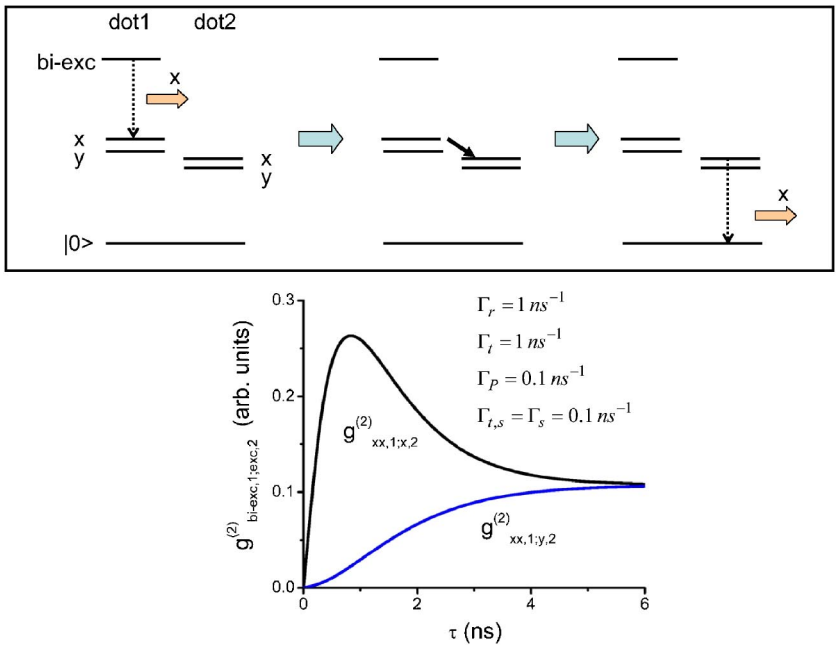

FIG. 8. (Color online) Upper part: schematics of processes contributing to the correlation function $g^{(2)}_{xx,1;x,2}$. In the first step, a biexciton in QD1 emits the x-photon; the second step is interdot transfer; the last step is emission of the x-photon by QD2. Lower part: calculated functions $g^{(2)}_{xx,1;x,2}$ and $g^{(2)}_{xx,1;y,2}$. Since interdot transfer mostly conserves spin, $g^{(2)}_{xx,1;x,2} > g^{(2)}_{xx,1;y,2}$. The parameters of relaxation are shown in the figure and correspond to a QD pair with $R=5$ nm, $d=0$, and $\Delta E \sim 2$ meV.

dence. Consider now the biexciton in QD1. It decays in a radiative cascade emitting two photons with the same polarizations (x, x or y, y photon pairs).[24] If the first emitted photon has the x-polarization, the remaining exciton in QD1 has the x-character. This exciton can recombine or can be transferred to QD2. Since the exciton spin is mostly conserved in the transfer process, we expect that QD2 will strongly radiate x-photons shortly after emission of the x-photon from QD1. This means that $g^{(2)}_{xx,1;x,2} > g^{(2)}_{xx,1;y,2}$, where the index xx labels the x-photon emitted by the biexciton in QD1. In other words, we use a biexciton in QD1 as a tool to prepare the x-exciton state at $\tau=0$. Then, the initial conditions at $\tau=0$ are $n_0=0$, $n_{\alpha,k}=1$ if $(\alpha,k)=(x,1)$ and 0 otherwise. Figure 8 demonstrates the striking difference between the polarized correlation functions ($g^{(2)}_{xx,1;x,2}$ and $g^{(2)}_{xx,1;y,2}$) in the important region $\tau>0$. In this way, by comparing $g^{(2)}_{xx,1;x,2}$ and $g^{(2)}_{xx,1;y,2}$, directional spin transfer between QDs can be observed experimentally.

V. STRONGLY RESONANT COULOMB TRANSFER

The convectional Förster mechanism is based on the resonance condition between the "donor" and "acceptor:"[3] the ground-state energy of the donor molecule coincides with the energy of an excited state of the acceptor. In the QD system, such a condition can be realized if the ground s-s exciton transition in the QD1 has the same energy as the p-p transition in QD2 (Fig. 9). Here s and p are the shell indexes in a QD. In this process, the s-exciton in QD1 is first transferred to the p-state of QD2; then it relaxes to the ground state of the QD2. The transfer rate of this process consists of two contributions:

$$W^{res}_{dot1\to dot2} = W^{ph} + W^{dir}, \tag{19}$$

where W^{ph} is the phonon-assisted transfer rate given by Eq. (16) in which ΔE is the energy difference between s- and p-excitons in QD1 and QD2, respectively. The rate W^{dir} describes direct resonant transfer between QDs. The latter can be calculated in the spirit of the convectional Förster theory as

$$W^{dir} = \frac{2\pi}{\hbar}|M_{dot1,\alpha\to dot2,\alpha'}|^2 J(\Delta E), \tag{20}$$

where $J(\Delta E)=1/\hbar\pi\Gamma_{en}/2/(\Delta E^2/\hbar^2+\Gamma^2_{en}/4)$ is the normalized effective density of states in the QD2, Γ_{en} is the energy relaxation rate in the QD2, and $\Delta E=E_{exc,dot1}-E_{exc,dot2}$. To obtain the equation (20) one should solve the master equation involving the density matrix and assume that $\hbar\Gamma_{en} > |M_{dot1\to dot2}|$. The latter condition can be easily satisfied because the excited p-states are quasistationary and the phonon-induced relaxation in QDs is fast usually; the typical relaxation times of self-assembled QDs are in the range of 50 ps.[23] In the opposite limit $\hbar\Gamma_{en} < |M_{dot1\to dot2}|$, the coupling between the ground s-state of QD1 and the excited p-state of QD2 is coherent; it has the character of Rabi oscillations. Then, in the case of $\hbar\Gamma_{en} < |M_{dot1\to dot2}|$, the characteristic time for transfer from the s-state of QD1 to the s-state of QD2 will be about $1/\Gamma_{en}$.

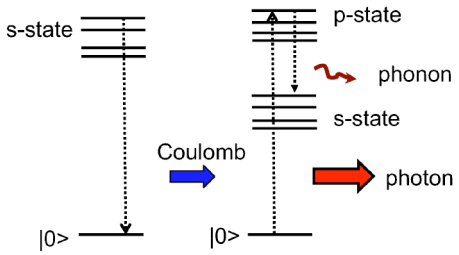

FIG. 9. (Color online) Resonant transfer process involving the s-state in QD1 and the p-state in QD2. Relaxation in QD2 is phonon-assisted.

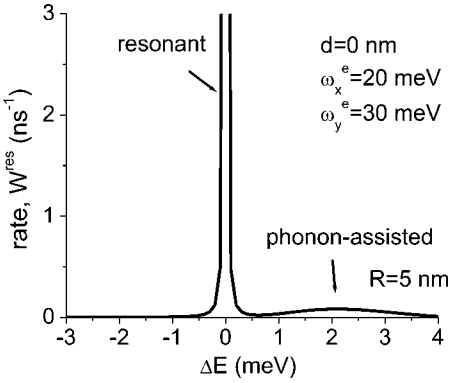

FIG. 10. Resonant transfer rate corresponding to the process shown in Fig. 8. The parameters of the QD pair are $R=5$, $\hbar\omega_x^e=20$ meV, $\hbar\omega_y^e=30$ meV, $d=0$, and $1/\Gamma_{en}=40$ ps. Temperature $T=4$ K. The exciton spin is conserved in the transfer process.

We now calculate the resonant transfer rate for typical parameters of self-assembled QDs. Again, the rate strongly depends on the resonance condition (see Fig. 10). The calculated rate demonstrates strong enhancement for $\Delta E \sim \hbar\Gamma_{en}$ and also has the structure due to the phonon-assisted processes discussed above.

The transfer rate W^{res} is proportional to $|M_{dot1,\alpha\to dot2,\alpha'}|^2$ and therefore the spin-selection rules are given by the Coulomb matrix elements. However, the complete transfer process contains energy relaxation inside QD2 (Fig. 9). This relaxation can lead to spin flip. Then, the efficiency of spin transfer will also depend on the ratio between intradot relaxation rates with and without spin flip. If energy relaxation inside QD2 involves mostly the heavy-hole states, spin-flip relaxation will be weak, since the main contributions to electron-phonon scattering are not spin-dependent and, simultaneously, the heavy-hole exciton functions are factorized.[21] It concerns both the acoustic-phonon interaction (15) and the Fröhlich scattering with emission of LO-phonons.[20] To conclude this section, we note that the resonant transfer process can involve a localized state in the wetting layer, instead of the *p*-state in QD2. Such a possibility was discussed in Ref. 5.

VI. DISCUSSION

In Secs. III and V, we discussed incoherent transfer assisted by phonons or involving a broadened state in QD2. The phonon-assisted transfer regime between ground states in QD1 and QD2 assumes that the energy difference ΔE is larger than the Coulomb matrix element $|M_{dot1\to dot2}|$. Now we briefly consider the case of coherent resonant coupling in the regime $\Delta E \sim |M_{dot1\to dot2}|$.[12–14] This regime requires fine-tuning of energies of QDs; this can be done, for example, with magnetic and electric fields. The QDs can be designed from different materials and therefore may have different *g*-factors. By changing a magnetic field, one can change ΔE. A similar principle can be used in the case of an applied electric field; if the QDs have different dipole moments, ΔE can be controlled by the electric field.

The calculated Coulomb matrix elements (see Fig. 4) are in the range of 0.05 meV for $R=5$ nm. The corresponding time is quite short: $\Delta t=\hbar/|M_{dot1\to dot2}|\sim 10$ ps. This time is much shorter than the typical recombination time of ground-state excitons in QDs, which is about 1 ns. Therefore the coherent Coulomb-induced coupling can exist in resonant pairs of QDs. In the case of $\Delta E=0$ and a QD molecule with $d=0$, the one-exciton wave functions are given by the linear combinations:

$$\Psi_x = \frac{|dot1,x\rangle|dot2,0\rangle \pm |dot1,0\rangle|dot2,x\rangle}{\sqrt{2}},$$

$$\Psi_y = \frac{|dot1,y\rangle|dot2,0\rangle \pm |dot1,0\rangle|dot2,y\rangle}{\sqrt{2}}. \qquad (21)$$

The energy splitting within the pairs of states is given by $2|M_{dot1\to dot2}|$. This energy can be regarded as a Rabi frequency. If the exciton is created initially in the QD1, the time to transfer the exciton to the neighboring dot would be $\Delta t=\hbar/|M_{dot1\to dot2}|\sim 10$ ps for the QD pair with $R=5$ nm. With increasing R, the transfer times will become longer. In the regime of coherent coupling, transfer of spin information occurs coherently, without any energy dissipation. The coherent spin-Rabi oscillations between QDs can probably be observed with modern optical methods.

To conclude, we have described the spin-dependent Coulomb interaction in a QD pair. Such a coupling suggests the possibility to transfer spin information between individual nanocrystals without transfer of charge or mass. The spin-dependent transfer originates from the exchange and spin-orbit interactions in semiconductors and strongly depends on symmetry and shapes of nanocrystals. If symmetry of a QD pair is high enough, spin information can be transferred without losses. If symmetry is broken, spin relaxation in the transfer process can become significant. To calculate the transfer rates in the realistic model, we use a generalized dipole-dipole approximation which is valid if $R \gg a_{\text{lattice}}$. The usual dipole-dipole approximation ($R \gg l_{dot}$) gives too large numbers for the realistic interdot distances. As a method to observe spin transfer, we consider spin-dependent photon correlations in a pair of QDs.

ACKNOWLEDGMENTS

The author would like to thank Pierre Petroff for some important comments and S. Ulloa, G. Bryant, B. McCombe, G. Medeiros-Ribeiro, M. Ouyang, and M. Bayer for helpful discussions. This work was supported by the CMSS Program at Ohio University and the AvH and Volkswagen Foundations.

[1] *Semiconductor Spintronics and Quantum Computation*, edited by D. D. Awschalom, D. Loss, and N. Samarth (Springer-Verlag, Berlin, 2002).
[2] A. O. Govorov, Phys. Rev. B **68**, 075315 (2003).
[3] Th. Förster, in *Modern Quantum Chemistry*, edited by O. Sinanoglu (Academic, New York, 1965).
[4] C. R. Kagan, C. B. Murray, and M. G. Bawendi, Phys. Rev. B **54**, 8633 (1996).
[5] B. Gerardot, S. Strauf, M. de Dood, A. Badolato, K. Hennessy, E. Hu, D. Bouwmeester, and P. M. Petroff (unpublished).
[6] G. Parascandolo and V. Savona, Phys. Rev. B **71**, 045335 (2005).
[7] R. Hanbury-Brown and R. Q. Twiss, Nature (London) **178**, 1447 (1956).
[8] A. J. Berglund, A. C. Doherty, and H. Mabuchi, Phys. Rev. Lett. **89**, 068101 (2002).
[9] M. Bayer, P. Hawrylak, K. Hinzer, S. Fafard, M. Korkusinski, Z. R. Wasilewski, O. Stern, and A. Forchel, Science **291**, 451 (2001); H. J. Krenner, M. Sabathil, E. C. Clark, A. Kress, D. Schuh, M. Bichler, G. Abstreiter, and J. J. Finley, Phys. Rev. Lett. **94**, 057402 (2005).
[10] M. Ouyang and D. D. Awschalom, Science **301**, 1074 (2003).
[11] F. Meier, V. Cerletti, O. Gywat, D. Loss, and D. D. Awschalom, Phys. Rev. B **69**, 195315 (2004).
[12] G. W. Bryant, Physica B **314**, 15 (2002).
[13] B. W. Lovett, J. H. Reina, A. Nazir, and G. A. Briggs, Phys. Rev. B **68**, 205319 (2003).
[14] A. N. Al-Ahmadi and S. E. Ulloa, Phys. Rev. B **70**, 201302(R) (2004).
[15] R. Leon, P. M. Petroff, D. Leonard, and S. Fafard, Science **267**, 1966 (1995); M. Grundmann, J. Christen, N. N. Ledentsov, J. Böhrer, D. Bimberg, S. S. Ruvimov, P. Werner, U. Richter, U. Gösele, J. Heydenreich, V. M. Ustinov, A. Yu. Egorov, A. E. Zhukov, P. S. Kop'ev, and Zh. I. Alferov, Phys. Rev. Lett. **74**, 4043 (1995).
[16] A. O. Govorov, R. J. Warburton, and K. Karrai, Phys. Rev. B **67**, 241307 (2003); C. Schulhauser, D. Haft, R. J. Warburton, K. Karrai, A. O. Govorov, A. V. Kalameitsev, A. Chaplik, W. Schoenfeld, J. M. Garcia and P. M. Petroff, *ibid.* **66**, 193303 (2002).
[17] D. Gammon, E. S. Snow, B. V. Shanabrook, D. S. Katzer, and D. Park, Phys. Rev. Lett. **76**, 3005 (1996); M. Bayer, A. Kuther, A. Forchel, A. Gorbunov, V. B. Timofeev, F. Schafer, J. P. Reithmaier, T. L. Reinecke, and S. N. Walck, *ibid.* **82**, 1748 (1999).
[18] E. L. Ivchenko and G. E. Pikus, *Superlattices and Other Heterostructures. Symmetry and Optical Phenomena* (Springer, Berlin, 1997).
[19] Our model does not include the heavy-light hole mixing which may involve dark states in transfer processes.
[20] G. D. Mahan, *Many-Particle Physics* (Plenum, New York, 2000).
[21] It is also important to note that the heavy-hole exciton states can be written as a product of the envelope function and the spin-dependent Bloch function, $|dotk\rangle = \phi_e(r_e)\phi_h(r_h)\chi_{exc}(r_e,\sigma_e,r_h,\sigma_h)$, where χ_{exc} is the Bloch function of an exciton. The electron-phonon operator in the matrix elements act only on the spin-independent envelope function $\phi_e(r_e)\phi_h(r_h)$ and therefore the phonon matrix elements are diagonal with respect to the exciton spin index α.
[22] P. Michler, A. Kiraz, C. Becher, W. V. Schoenfeld, P. M. Petroff, Lidong Zhang, E. Hu, and A. Imamoglu, Science **290**, 2282 (2000).
[23] This time is of order of the time to trap an electron-hole pair into the ground state of a QD and is typically short.
[24] S. M. Ulrich, S. Strauf, P. Michler, G. Bacher and A. Forchel, Appl. Phys. Lett. **83**, 1848 (2003).